

A diacylglycerol kinase modulates long-term thermotactic behavioral plasticity in *C. elegans*

David Biron^{1,2}, Mayumi Shibuya², Christopher Gabel¹, Sara M Wasserman², Damon A Clark¹, Adam Brown^{2,3}, Piali Sengupta² & Aravinthan D T Samuel¹

A memory of prior thermal experience governs *Caenorhabditis elegans* thermotactic behavior. On a spatial thermal gradient, *C. elegans* tracks isotherms near a remembered temperature we call the thermotactic set-point (T_S). The T_S corresponds to the previous cultivation temperature and can be reset by sustained exposure to a new temperature. The mechanisms underlying this behavioral plasticity are unknown, partly because sensory and experience-dependent components of thermotactic behavior have been difficult to separate. Using newly developed quantitative behavioral analyses, we demonstrate that the T_S represents a weighted average of a worm's temperature history. We identify the DGK-3 diacylglycerol kinase as a thermal memory molecule that regulates the rate of T_S resetting by modulating the temperature range of synaptic output, but not temperature sensitivity, of the AFD thermosensory neurons. These results provide the first mechanistic insight into the basis of experience-dependent plasticity in this complex behavior.

A major goal in neuroscience is to elucidate the molecular and neural bases of experience-dependent adaptive behavior. Adaptive changes in behavior have been associated with alterations in neuron and neural circuit functions, most notably in the gill withdrawal reflex in *Aplysia*^{1–3}. Although functional changes in sensory neurons can contribute to both short- and long-term behavioral plasticity in *Aplysia*^{4,5}, long-term behavioral plasticity in other systems has generally been attributed to alterations in synaptic strengths and connectivity at higher processing centers^{6–8}, and the contribution of sensory neurons to long-term changes in behavior remains relatively unexplored.

C. elegans shows a variety of behaviors that are modulated by environmental conditions and previous experience⁹. The *C. elegans* nervous system is compact, and the synaptic connectivities of all neurons have been anatomically mapped¹⁰. Moreover, the contributions of individual molecules and neurons to specific behaviors have been defined through genetic and laser ablation studies⁹. Taken together with recent advances in the quantitative analysis of *C. elegans* behavior and the development of physiological methods to analyze neuronal activity^{11–16}, these features now make *C. elegans* an ideal model organism in which to investigate the roles of genes, neurons and neuronal circuits in regulating behavior and behavioral plasticity.

Thermotaxis is a particularly sophisticated, experience-dependent behavior in *C. elegans*¹⁷. The behavior of *C. elegans* on spatial thermal gradients is governed by a memory of its previous cultivation temperature¹⁷. When *C. elegans* navigates spatial thermal gradients at temperatures above its previous cultivation temperature, it crawls down the gradients in what is called cryophilic movement. When

navigating within 2–3 °C of its previous cultivation temperature, *C. elegans* tracks isotherms in markedly persistent periods of forward movement¹⁷. Thus, *C. elegans* effectively compares the ambient temperature with a memory of its previous cultivation temperature to enact different strategies to navigate thermal gradients. The memory of cultivation temperature retains plasticity in the adult stage, and it can be reset by cultivating adult worms at one temperature and then shifting them to a new temperature for a sustained period¹⁷. The adaptability of thermotactic navigation may be a behavioral component of heterothermal acclimation in *C. elegans*, a common phenomenon in ectothermic animals, contributing to their ability to compensate for prolonged changes in the temperatures of their environments¹⁸.

Genetic and physical lesions of the bilateral AFD neurons have been shown to disrupt thermotactic behavior, including the ability to track isotherms^{15,19,20}, implying that the AFD neurons are thermosensory. Recent physiological measurements have also shown that patterns of AFD neuronal activity are correlated with the previous cultivation temperature^{21–23}. These observations indicate that the memory of cultivation temperature may be at least partly encoded in patterns of AFD neuronal activity^{21–23}. However, the molecules and mechanisms required for the storage and resetting of this memory are unknown.

Here, we use quantitative behavioral analyses to demonstrate that the cultivation temperature memory in *C. elegans* represents a weighted average of the worm's temperature history. We find that mutations in the *dgk-3* diacylglycerol kinase gene result in defects in resetting this form of long-term thermal memory. We show that

¹Department of Physics, Harvard University, 17 Oxford Street, Cambridge, Massachusetts 02138, USA. ²Department of Biology and National Center for Behavioral Genomics, 415 South Street, Brandeis University, Waltham, Massachusetts 02454, USA. ³Present address: Broad Institute, 320 Charles Street, Cambridge, Massachusetts 02141, USA. Correspondence should be addressed to P.S. (sengupta@brandeis.edu) or A.D.T.S. (samuel@physics.harvard.edu).

Received 6 June; accepted 10 October; published online 5 November 2006; doi:10.1038/nn1796

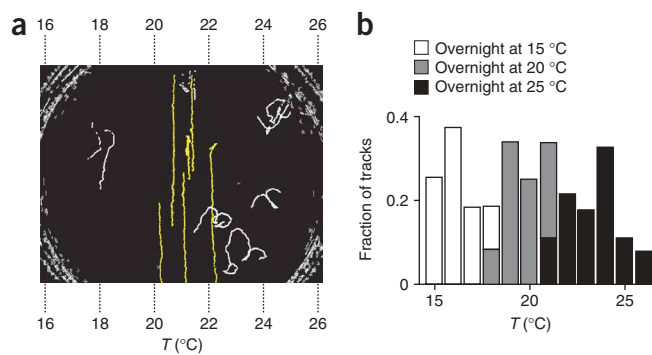


Figure 1 *C. elegans* track isotherms around a thermotactic set point (T_S) corresponding to their cultivation temperature. (a) Isothermal tracks made by wild-type worms cultivated overnight at 20 °C and placed on a thermal gradient. Snapshots of the movement of worms on the gradient were digitized and overlaid such that their trajectories were visible. We defined isothermal tracks, artificially colored yellow, as long vertical trajectories (see Methods). White curved lines are trajectories that were made by worms not tracking isotherms at any given time, typically at temperatures far from the T_S . (b) The distributions (superimposed rather than stacked) of the temperatures at which wild-type worms tracked isotherms after overnight cultivation at 15 °C, 20 °C and 25 °C. The center of each distribution is close to the overnight cultivation temperature of the worms. $n = 20$ –30 each.

DGK-3 affects the resetting of the thermal memory by altering plasticity in the temperature range of AFD synaptic output, without detectably affecting plasticity in the temperature range of AFD temperature sensitivity. Our observations indicate that adaptive changes in sensory neuron function mediate long-term thermotactic behavioral plasticity in *C. elegans* and implicate a diacylglycerol kinase as a key regulator of this process.

RESULTS

Temperature history is integrated to generate the T_S

When placed on a spatial thermal gradient, *C. elegans* tracks isotherms within 2–3 °C of its previous cultivation temperature (Fig. 1)^{17,24}. Thus, when a population of worms is placed on a steep spatial thermal gradient and allowed to crawl freely for several minutes, isothermal tracks emerge as persistent periods of forward movement in a direction perpendicular to the temperature gradient (Supplementary Video 1 online). Since these isothermal tracks only emerge in the narrow band of temperatures around the remembered cultivation temperature¹⁷, the cultivation temperature memory can be accurately quantified by measuring the average temperature of isothermal tracks shown by a population of worms in a short interval of time. We refer to this behavioral metric of cultivation temperature memory as the thermotactic set-point (T_S).

We quantified the rate of T_S resetting by cultivating worms overnight at 15 °C or 25 °C and shifting them to 25 °C or 15 °C, respectively, for different periods of time (Fig. 2a–d). We found that T_S resetting from the overnight cultivation temperature to the new temperature followed a roughly exponential time-course with time constants of 1.6 ± 0.2 h and 1.8 ± 0.2 h for temperature upshift and downshift assays, respectively (Fig. 2c,d). Thus, at intermediate time points, worms tracked isotherms near temperatures they experienced only transiently during the equilibration of the cultivation plate to the new temperature (Fig. 2a–d).

The thermotactic set-point in *C. elegans* has been suggested to require associative learning between temperature and food-dependent cues^{17,25,26}. However, we found that the rate of T_S resetting to new temperatures was unaffected by the absence of food at the new temperature (Fig. 2e,f). We conclude that long-term plasticity in the temperature range of isothermal tracking does not involve association between temperature and food, and that the T_S reflects a simple integration over temperature history.

The roughly exponential relaxation of the T_S to new temperatures implies that the dynamics of T_S resetting is approximated by first-order kinetics:

$$\frac{dT_S}{dt} = \frac{1}{\tau_{\text{up,dn}}} (T - T_S) \quad (1)$$

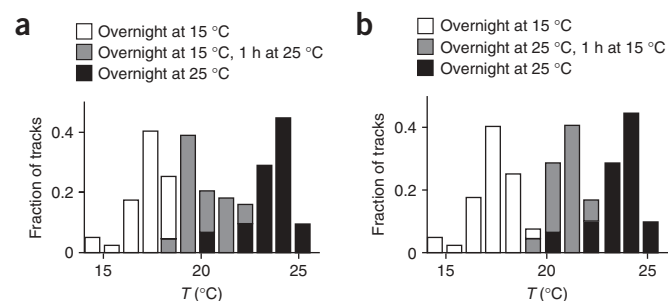
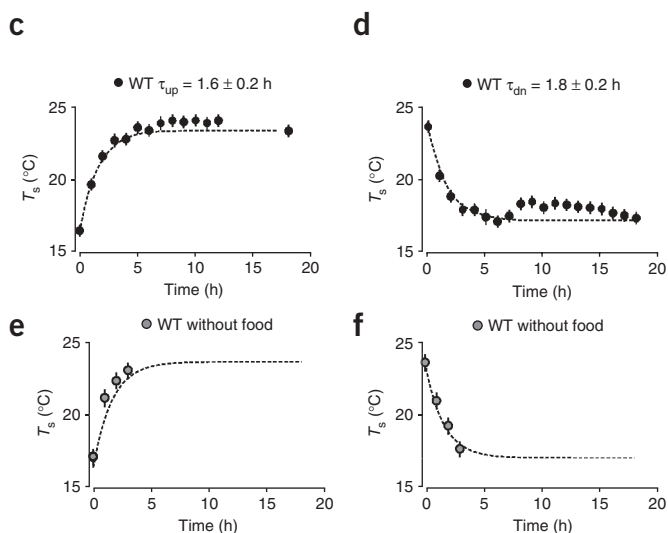
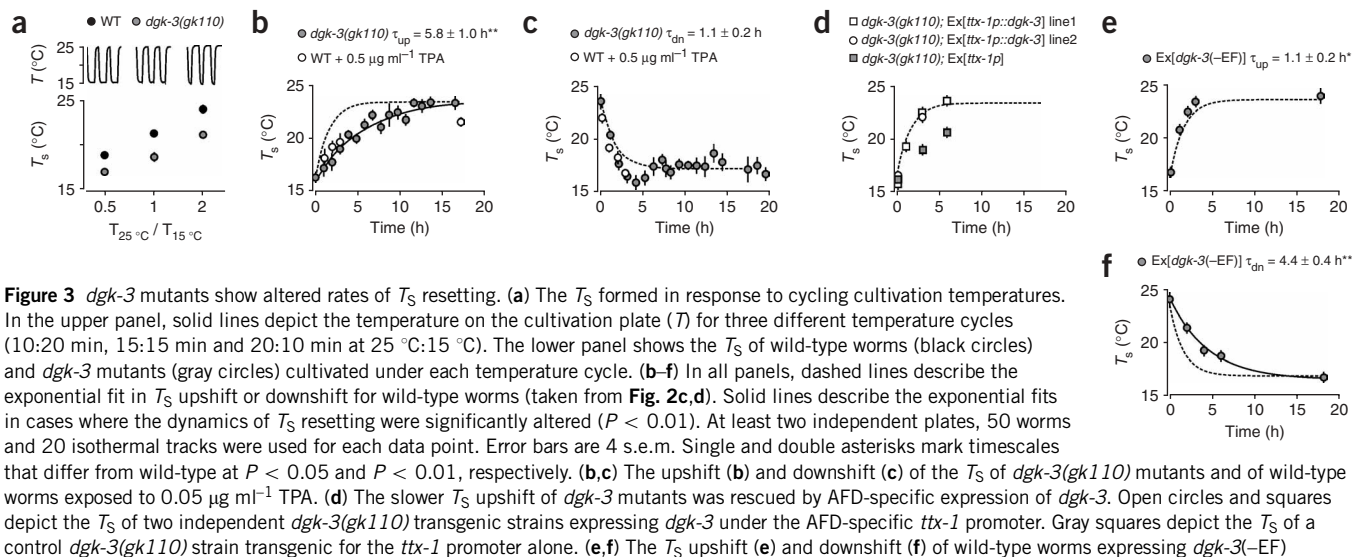


Figure 2 The T_S represents an average of a worm's temperature history, and T_S resetting does not depend on the presence of bacterial food. (a,b) The distributions of the temperatures at which wild-type worms track isotherms after being cultivated overnight at 15 °C (plotted in both a and b to facilitate comparison), at 25 °C (also a,b), overnight at 15 °C followed by cultivation for 1 h at 25 °C (a), and overnight at 25 °C followed by cultivation for 1 h at 15 °C (b). (c,d) The upshift (c) and downshift (d) of the T_S of wild-type worms in the presence of food as measured in upshift and downshift tracking assays, respectively (see Methods). The circles represent experimental data, and the dashed lines indicate exponential fits. (e,f) The T_S upshift (e) and downshift (f) of wild-type worms in the absence of food. Tracking behavior weakened after 3 h of starvation and was not followed further. Dashed lines indicate the exponential fits to the wild-type behavior from (c) and (d). At least two independent plates, 50 worms and 20 isothermal tracks were used for each data point. Error bars are 4 s.e.m. (so that they show clearly).





where T is the temperature of the environment and τ_{up} and τ_{dn} are the time constants for shifting T_S when $T > T_S$ or $T < T_S$, respectively. Equation (1) implies that if the worms are cultivated in an environment that cycles rapidly between 15 °C and 25 °C, then the T_S will form at an intermediate temperature, weighted toward higher or lower temperatures by the relative values of τ_{up} and τ_{dn} as well as the relative time intervals spent at 15 °C and 25 °C in the cycle. To test this hypothesis, we cultivated worms overnight in a temperature cycle alternating between fixed time intervals at 15 °C and at 25 °C, both intervals being shorter than τ_{up} and τ_{dn} (Fig. 3a). Indeed, we found that the T_S formed at an intermediate temperature, although at a temperature slightly higher than that predicted by equation (1). These results indicate that worms have distinct values of T_S at all times, which correspond to weighted averages of their previous cultivation temperatures.

The rate of T_S resetting is altered in *dgk-3* mutants

To identify molecules that contribute to *C. elegans* thermotaxis, we previously identified genes preferentially expressed in the AFD neurons by expression profiling²⁷. Of this set, the *dgk-3* gene, encoding a diacylglycerol (DAG) kinase (DGK), was expressed in AFD and in a small subset of additional sensory neurons. We found that *dgk-3* null mutant worms showed thermotaxis in a superficially wild-type manner; after overnight cultivation at a specific temperature, *dgk-3* null mutants tracked isotherms near that cultivation temperature and showed cryophilic movement at higher temperatures (Fig. 3b,c and data not shown). However, we found that *dgk-3* mutants reset their T_S at a significantly slower rate than wild-type worms when shifted from 15 °C to 25 °C (Fig. 3b), such that shortly after the shift, *dgk-3* mutants consistently tracked isotherms at lower temperatures than did wild-type worms. This defect was rescued by expressing a *dgk-3* cDNA specifically in the AFD neurons, indicating that DGK-3 acts in the AFD neurons to modulate the dynamics of T_S resetting (Fig. 3d). When we shifted *dgk-3* null mutants from 25 °C to 15 °C, *dgk-3* mutants again tracked isotherms at slightly lower temperatures than those tracked by wild-type worms shortly after the shift, although the difference in the overall time course of T_S resetting was less marked (Fig. 3c). Therefore, after sustained exposure to new temperatures, *dgk-3* mutants showed defects specifically in the dynamics of T_S resetting, although eventually

these worms showed the same T_S as wild-type worms. As expected based on the experimentally measured τ_{up} and τ_{dn} time constants of *dgk-3* mutants, *dgk-3* null mutants formed their T_S at lower temperatures than did wild-type worms when cultivated with cycling temperatures (Fig. 3a).

dgk-3 encodes the *C. elegans* ortholog of the mammalian DGK- β enzyme, and it has previously been implicated in the regulation of olfactory adaptation behaviors²⁸. Members of the DGK- α , DGK- β and DGK- γ kinase families contain two calcium-binding EF-hand motifs (Supplementary Fig. 1 online), which can be autoinhibitory in the absence of calcium^{29–31}. Deletion of the EF-hand motifs has been shown to increase the enzymatic functions of DGK- α (refs. 32,33). To determine the effects of a similar deletion on the functions of DGK-3, we expressed a *dgk-3* cDNA lacking the EF hands (DGK-3(-EF)) in the AFD neurons of wild-type worms. The thermotactic behavior of the transgenic worms was superficially normal, but they showed slightly faster resetting of T_S when shifted from 15 °C to 25 °C and significantly slower resetting of T_S when shifted from 25 °C to 15 °C (Fig. 3e,f). Thus, in contrast to worms carrying *dgk-3* null mutations, which track isotherms at temperatures lower than wild-type during resetting T_S to new temperatures, worms expressing *dgk-3(-EF)* track isotherms at temperatures higher than wild-type during resetting to new temperatures.

DGKs contribute to intracellular biochemical signaling pathways by lowering the levels of the phospholipid second messenger DAG via phosphorylation and conversion of DAG to phosphatidic acid³⁴. We speculated that the reduced rate of T_S resetting toward higher temperatures in the *dgk-3* null mutants might be due to higher concentrations of DAG. Indeed, we found that adding the DAG analog 12-*O*-tetradecanoylphorbol-13-acetate (TPA) to wild-type worms that were shifted from 15 °C to 25 °C or from 25 °C to 15 °C phenocopied the effects of the *dgk-3* mutation, causing the worms to consistently track isotherms at lower temperatures during the time-course of T_S resetting (Fig. 3b,c). Taken together, these results indicate that levels of DGK-3 enzymatic activity, and in particular the levels of DAG in the AFD neurons, affect the rates of thermal memory resetting. We explored the possibility that DGK-3 activity is regulated by temperature-dependent transcription of the *dgk-3* gene by quantifying GFP fluorescence in the AFD and AWC neurons of transgenic worms expressing a *dgk-3::gfp* fusion gene. However, GFP fluorescence was not significantly altered in

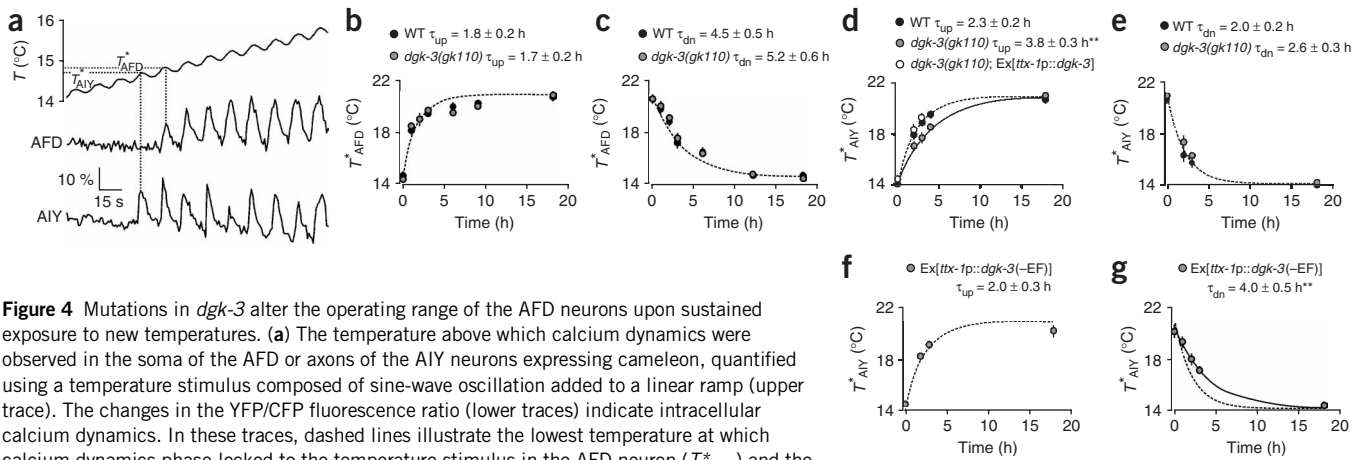


Figure 4 Mutations in *dgk-3* alter the operating range of the AFD neurons upon sustained exposure to new temperatures. (a) The temperature above which calcium dynamics were observed in the soma of the AFD or axons of the AIY neurons expressing cameleon, quantified using a temperature stimulus composed of sine-wave oscillation added to a linear ramp (upper trace). The changes in the YFP/CFP fluorescence ratio (lower traces) indicate intracellular calcium dynamics. In these traces, dashed lines illustrate the lowest temperature at which calcium dynamics phase-locked to the temperature stimulus in the AFD neuron (T^*_{AFD}) and the AIY neuron (T^*_{AIY}). (b–g) The time course of T^*_{AFD} and T^*_{AIY} resetting, quantified in upshift and downshift experiments. Each data point represents an average of $n = 6–11$ worms, and the error bars are 4 s.e.m. In each panel, dashed lines represent exponential fits to wild-type data. Double asterisks indicate timescales that differ from wild-type at $P < 0.01$, with solid lines representing the exponential fits to these mutant data. (b,c) The T^*_{AFD} upshift and downshift of *dgk-3* null mutant worms are unaffected. (d) The T^*_{AIY} upshift of *dgk-3* null mutants is slow and is rescued by cell-specific expression of *dgk-3*. (e) The T^*_{AIY} downshift of *dgk-3* null mutants is unaffected. (f) The T^*_{AIY} upshift of *tx-1p::dgk-3(-EF)*-expressing worms is unaffected. (g) The T^*_{AIY} downshift of *tx-1p::dgk-3(-EF)*-expressing worms is slow. The T^*_{AIY} downshift of control worms transgenic for the coinjection marker and the empty expression vector alone is unaffected (data not shown).

either neuron type in worms cultivated at 15 °C or 25 °C (data not shown). Therefore, DGK-3 enzymatic activity in the AFD neuron may be directly regulated by thermosensory signal transduction pathways.

DGK-3 regulates plasticity in AFD synaptic output

The defect in behavioral plasticity observed in *dgk-3* mutants might be a consequence of defects at one or more levels of AFD neuronal function, including temperature detection or synaptic output. Stimulation of the AFD neurons by temperature inputs can be monitored by imaging intracellular calcium concentrations in AFD using the calcium-binding fluorescent protein cameleon expressed under an AFD-specific promoter³⁵. Recently, we and others showed that intracellular calcium dynamics in AFD are sensitive to temperature changes only at temperatures above a certain lower bound (T^*_{AFD})^{21,22}. At temperatures above T^*_{AFD} , AFD calcium dynamics phase-lock to an oscillatory temperature input. At temperatures below T^*_{AFD} , temporal changes in temperature do not evoke intracellular calcium dynamics in AFD (Fig. 4a). In addition, we showed that T^*_{AFD} for wild-type worms was approximately 15 °C, 17 °C and 21 °C for worms cultivated overnight at 15 °C, 20 °C and 25 °C, respectively²². We also showed that both calcium dynamics and T^*_{AFD} could be measured at the sensory endings of the AFD neurons²², indicating that AFD neuronal plasticity may be partly reflected in thermoreceptor sensitivity. Thus, long-term changes in the behavioral metric T_S parallel long-term changes in the physiological metric T^*_{AFD} , although the precise correspondence between AFD activity and isothermal tracking behavior has not yet been firmly established.

To measure the dynamics of T^*_{AFD} resetting, and to determine whether these dynamics were altered in *dgk-3* mutants, we cultivated wild-type worms and *dgk-3* null mutants expressing cameleon in their AFD neurons and performed temperature upshift and downshift assays. The dynamics in T^*_{AFD} were measured by subjecting individual worms to a temperature stimulus composed of a rapid sinusoidal oscillation added to a positive linear ramp, and recording the lowest temperature that evoked calcium dynamics (Fig. 4a). We observed gradual upward and downward shifts in T^*_{AFD} after temperature

upshifts and downshifts that were similar to the gradual shifts in T_S that we measured in behavioral experiments (Fig. 4b,c). However, the dynamics of T^*_{AFD} resetting were unaltered in *dgk-3* mutants (Fig. 4b,c), indicating that DGK-3 may not directly affect plasticity in the temperature range of AFD thermoreceptor sensitivity.

In our earlier study, we also demonstrated that calcium dynamics in the processes of the AIY neurons, the postsynaptic partners of AFD, are driven by synaptic output of AFD during an oscillating temperature input²². Similarly to the observed calcium dynamics in the AFD neurons, at temperatures above a certain lower bound (T^*_{AIY}), calcium dynamics in the AIY process phase-locked to the oscillatory component of a temperature input (Fig. 4a). The T^*_{AIY} for wild-type worms was approximately 15 °C, 17 °C and 21 °C for worms cultivated overnight at 15 °C, 20 °C and 25 °C, respectively²². Thus, long-term changes in T^*_{AIY} also parallel long-term changes in thermotactic behavior. Next, we quantified the dynamics of T^*_{AIY} resetting in wild-type worms and *dgk-3* null mutants after temperature upshifts and downshifts. Similarly to T^*_{AFD} , T^*_{AIY} reset with an exponential time course paralleling the observed behavioral plasticity (Fig. 4d,e). Notably, the rate of T^*_{AIY} resetting toward higher temperatures of *dgk-3* null mutants was significantly slower than that of wild-type worms, whereas the rate of T^*_{AIY} resetting toward lower temperatures appeared to be unaltered (Fig. 4d,e). Thus, the *dgk-3* null mutation has similar effects on the plasticity of both the temperature range of AFD synaptic output and the isothermal tracking behavior. We verified that AFD-specific expression of *dgk-3* rescued the effect on T^*_{AIY} resetting (Fig. 4d). Finally, we quantified the rate of T^*_{AIY} resetting in worms overexpressing *dgk-3(-EF)* in the AFD neurons: we found that these strains showed slowed rates of T^*_{AIY} resetting toward lower temperatures (Fig. 4f,g), in parallel to their slowed rates of T_S resetting toward lower temperatures in behavioral assays (Fig. 3e,f).

DISCUSSION

Thermotaxis in *C. elegans* is an attractive model system for studying long-term plasticity at the molecular, neuronal and behavioral levels. The thermotactic behaviors of *C. elegans* are remarkably sophisticated,

involving both a cryophilic mode of behavior that enables the worm to crawl down thermal gradients when navigating at temperatures above the T_S and an isothermal tracking mode of behavior that is shown near the T_S ¹⁷. To rigorously analyze the mechanisms that mediate plasticity in *C. elegans* thermotaxis, it is necessary to implement assays that identify and quantitatively compare each component of thermosensory response and neuronal and behavioral plasticity. Here, we focused our attention on the worm's ability to reset the long-term thermal memory that determines the temperature range of its isothermal tracking behavior after sustained exposure to new temperatures. Measurement of the average temperatures of isothermal tracking affords a simple, robust and quantitative metric of behavioral plasticity, which may be attributed to plasticity in the temperature range of AFD temperature sensitivity, synaptic output or both. Although the molecules that mediate thermoreception in *C. elegans* remain to be identified, we have demonstrated that the DGK-3 diacylglycerol kinase acts in the AFD neurons to contribute to long-term plasticity by altering the temperature range of AFD synaptic output.

At temperatures above the lower bound T_{AFD}^* , thermoreceptor activity in the AFD neurons appears to trigger an increase in intracellular calcium concentrations. The *tax-2*- and *tax-4*-encoded cyclic nucleotide-gated channels have been implicated in AFD thermosensation^{21,36,37}, indicating that calcium influx through these channels may have a role in regulating AFD calcium dynamics. At temperatures above the lower bound T_{AIY}^* , thermoreceptor activity in AFD drives synaptic output to the AIY interneuron. The simplest interpretation of our observations is that plasticity in the behavioral metric T_S is related to plasticity in the physiological metrics T_{AFD}^* and T_{AIY}^* . Our results indicate that DGK-3 may affect T_{AIY}^* resetting without necessarily altering T_{AFD}^* , indicating that DGK-3 acts downstream of or in parallel to the calcium dynamics that we detected in AFD, and that multiple mechanisms within AFD contribute to AFD neuronal plasticity. DGKs have important roles in cellular signaling by lowering levels of DAG, a phospholipid second messenger that is produced in response to extracellular signals³⁴. In other systems, DAG has been shown to have multiple roles, including triggering downstream signaling cascades, activating protein kinase C and enhancing synaptic transmission through the synaptic vesicle priming protein UNC-13, as well as directly gating transient receptor potential (TRP) channels^{38–42}. In *Drosophila* photoreceptor cells and in *C. elegans* olfactory neurons, loss of DGK function has been shown to cause defects in signal termination and in adaptation to sensory stimuli^{28,43}.

Based on prior descriptions of DGK function and our observations, we propose a simple model for AFD-mediated plasticity in thermotactic behavior. We suggest that the temperature range of AFD neuronal function, defined as activation of both thermosensory and synaptic output properties, has a key role in regulating the temperature range of isothermal tracking. At temperatures above T_{AFD}^* , increases in temperature drive increases in intracellular calcium concentration in AFD, activating DGK-3 and lowering intracellular levels of DAG, which in turn affects the threshold of triggering AFD synaptic output measured as T_{AIY}^* . Increased levels of DAG, as in *dgk-3* null mutants, or addition of TPA to wild-type worms, may lower the threshold for triggering AFD synaptic output, resulting in lower temperatures for T_{AIY}^* and for isothermal tracking. Conversely, in *dgk-3(-EF)*-expressing worms, the lowered levels of DAG may increase the threshold for AFD synaptic output, resulting in higher temperatures for T_{AIY}^* and for isothermal tracking. Although we have not yet identified the cellular target of DAG in AFD, these results implicate the AFD sensory neurons as a locus of long-term plasticity in regulating *C. elegans* isothermal tracking behavior.

We note that there is unlikely to be a simple one-to-one correspondence between AFD activity and isothermal tracking behavior. The operating range of the AFD neuron—quantified by the range of temperatures in which temperature dynamics evoke calcium transients in AFD and AIY—spans the temperature range both of isothermal tracking and of cryophilic movement. Whereas our physiological metrics T_{AFD}^* and T_{AIY}^* appear to be near the lowest temperatures at which an individual worm may track isotherms, our behavioral metric T_S quantifies the middle of the temperature range of isothermal tracking behavior. Moreover, although AFD is so far the only sensory neuron to be linked to thermotaxis, other sensory neurons may also have roles in isothermal tracking behavior as well as in long-term behavioral plasticity.

Ectotherms have a diverse repertoire of responses to prolonged changes in ambient temperature, including behavioral, structural, physiological and biochemical adaptations. In particular, remodeling of membrane lipids has a critical role in the acclimation of ectotherms to varying temperatures, allowing cell membranes to maintain a relatively constant physical state across broad temperature ranges^{44,45}. Here, we have shown that DGK-3 regulates adaptation in *C. elegans* thermotactic behavior by regulating the temperature range of AFD synaptic output via modulation of levels of the DAG lipid second messenger. These observations raise the possibility that physiological mechanisms such as changes in membrane lipid composition may underlie additional aspects of thermal acclimation in the AFD and other neurons, thereby allowing thermotactic behavioral adaptation.

Other signal transduction molecules have been reported to affect thermotactic behavior in *C. elegans*, but with less certainty in their neuronal correlates. Mutations in a number of genes, including *dgk-1*, encoding DGK- α (refs. 46,47); *gcy-8*, -18 and -23, encoding guanylyl cyclases⁴⁸; *tax-6*, encoding a calcineurin subunit⁴⁹; and *ttx-4*, encoding novel protein kinase C (ref. 46), have been reported to result in altered thermosensory behaviors, but the neural mechanisms giving rise to the observed behavioral defects have not been defined. Overexpression of the NCS-1 neuronal calcium sensor in the AIY neurons was shown to affect the rate at which *C. elegans* resets its thermotactic preference, but the role of the endogenous gene is unclear⁵⁰. The characterization of the role of DGK-3 in long-term plasticity allows us to begin to dissect the pathways that give rise to adaptive behavior in *C. elegans*.

METHODS

Strains. The *dgk-3(gk110)* strain was outcrossed five times before analysis. A strain expressing cameleon (YC2.12) in the AFD neurons under the *nhr-38* promoter²¹ was a gift (see Acknowledgments). We generated transgenic strains using *unc-122::rfp* as the coinjection marker. We injected expression constructs at concentrations of 30–50 ng μl^{-1} . In all applicable cases, expression from the same extrachromosomal array was examined in wild-type and *dgk-3(gk110)* worms.

Molecular biology. We obtained the *dgk-3* cDNA from Open BioSystems, and corrected PCR-induced mutations present in the open reading frame by site-directed mutagenesis. *ttx-1p::dgk-3* was generated by cloning the *dgk-3* cDNA downstream of the *ttx-1* promoter in a *C. elegans* expression vector. Cameleon was expressed in the AIY interneurons by cloning YC2.12 sequences downstream of the *ttx-3* promoter in a *C. elegans* expression vector. The *dgk-3(-EF)* cDNA, encoding DGK-3_{174–247}, was generated by amplification and expressed under the *ttx-1* promoter. We confirmed all constructs by sequencing.

Tracking assays. We cultivated young adults overnight at 15°C or 25°C and then transferred them as young adults to 25°C or 15°C, respectively, for fixed intervals of time. We then transferred them within 7–10 min onto a 9-cm-diameter plate without bacterial food. The temperatures at the edges of the agar surface of an identical plate on a steep spatial thermal gradient were measured

before each assay. We placed the plate containing the worms on the gradient and left it to equilibrate for 5 min, and then recorded the worm movements for an additional 25 min. The horizontal positions of isothermal tracks were scored manually for each 5-min segment of the 25-min movie.

We defined isothermal tracks as straight vertical trajectories that were significantly longer (typically longer than 2 cm) than the persistent vertical distance traversed by worms at temperatures far from the T_S . The T_S for each set of conditions was measured as an average of tracking temperatures from at least two independent plates. In order to achieve rapid temperature cycles in the cycling cultivation temperature assay, we cultivated the worms on a thin agar layer (5 ml agar on a 9-cm-diameter plate) that was placed on an electronically temperature-controlled brass surface. We used glycerol to achieve a good thermal contact between the plate and the surface, and measured the temperature on the plate for several cycles before the overnight cultivation of the worms.

Calcium imaging. We glued a single young adult worm to a thin agar pad with cyanoacrylate glue (Abbott Laboratories) and monitored its temperature with a 200- μ m thermocouple (Physitemp) that was placed within 1–3 mm of the worm on the agar surface. We placed a coverslip over the worm and the thermocouple, and then placed the agar pad on a temperature control apparatus. We imaged calcium dynamics in a single neuron within 7–10 min of removing the worm from the incubator, allowing one measurement per worm. We did not observe any differences in calcium dynamics between the AFDL and AFDR neurons. Consequently, we typically focused on the neuron closest to the objective. The fluorescence of cameleon expressed in the AFD and AIY neurons was imaged using a Nikon $\times 40$ air objective (0.95 numerical aperture) and a Photometrics CoolSNAP camera. The yellow and cyan emissions of cameleon were split onto a single CCD chip. Exposure times ranged from 250 to 600 ms at a 1 Hz frame rate. We carried out image processing and analysis using MATLAB (Mathworks).

Note: Supplementary information is available on the Nature Neuroscience website.

ACKNOWLEDGMENTS

We are very grateful to C. Gauthier for technical assistance, the *Caenorhabditis* Genetics Center for strains, the *C. elegans* Gene Knockout Consortium for the *dgk-3(gk110)* allele, I. Mori (Nagoya University) for the *nhr-38::YC2*. 12-expressing transgenic strain, H. Suzuki (University of California, San Diego) for the YC2.12 clone, A. Fire (Stanford University) for the *C. elegans* expression vectors, and C. Bargmann, L. Griffith, O. Hobert, M. Rosbash and the Sengupta and Samuel labs for discussion and comments on the manuscript. This work was supported by a Human Frontier Science Program cross-disciplinary fellowship (D.B.), the US National Institutes of Health (NS44232, P.S.), and the US National Science Foundation, the McKnight Foundation and the Sloan Foundation (A.D.T.S.).

AUTHOR CONTRIBUTIONS

D.B. conducted the behavioral and imaging experiments. M.S., S.M.W., A.B. and P.S. conducted the molecular biology and genetic experiments. C.G. and D.A.C. developed the behavioral and imaging assays. A.B. and C.G. initially noted the *dgk-3* mutant phenotype. D.B., A.D.T.S. and P.S. contributed to data analysis and manuscript preparation.

COMPETING INTERESTS STATEMENT

The authors declare that they have no competing financial interests.

Published online at <http://www.nature.com/natureneuroscience>

Reprints and permissions information is available online at <http://npg.nature.com/reprintsandpermissions/>

- Castellucci, V.F., Carew, T.J. & Kandel, E.R. Cellular analysis of long-term habituation of the gill-withdrawal reflex of *Aplysia californica*. *Science* **202**, 1306–1308 (1976).
- Castellucci, V., Pinsker, H., Kupfermann, I. & Kandel, E.R. Neuronal mechanisms of habituation and dishabituation of the gill-withdrawal reflex in *Aplysia*. *Science* **167**, 1745–1748 (1970).
- Castellucci, V.F. & Kandel, E.R. A quantal analysis of the synaptic depression underlying habituation of the gill-withdrawal reflex in *Aplysia*. *Proc. Natl. Acad. Sci. USA* **71**, 5004–5008 (1974).
- Bailey, C.H. & Chen, M. Morphological basis of short-term habituation in *Aplysia*. *J. Neurosci.* **8**, 2452–2459 (1988).
- Bailey, C.H. & Chen, M. Morphological basis of long-term habituation and sensitization in *Aplysia*. *Science* **220**, 91–93 (1983).

- Bliss, T.V. & Lomo, T. Long-lasting potentiation of synaptic transmission in the dentate area of the anaesthetized rabbit following stimulation of the perforant path. *J. Physiol. (Lond.)* **232**, 331–356 (1973).
- Dudek, S.M. & Bear, M.F. Homosynaptic long-term depression in area CA1 of hippocampus and effects of *N*-methyl-D-aspartate receptor blockade. *Proc. Natl. Acad. Sci. USA* **89**, 4363–4367 (1992).
- Yu, D., Ponomarev, A. & Davis, R.L. Altered representation of the spatial code for odors after olfactory classical conditioning; memory trace formation by synaptic recruitment. *Neuron* **42**, 437–449 (2004).
- de Bono, M. & Maricq, A.V. Neuronal substrates of complex behaviors in *C. elegans*. *Annu. Rev. Neurosci.* **28**, 451–501 (2005).
- White, J.G., Southgate, E., Thomson, J.N. & Brenner, S. The structure of the nervous system of the nematode *Caenorhabditis elegans*. *Phil. Trans. R. Soc. Lond. B* **314**, 1–340 (1986).
- Goodman, M.B., Hall, D.H., Avery, L. & Lockery, S.R. Active currents regulate sensitivity and dynamic range in *C. elegans* neurons. *Neuron* **20**, 763–772 (1998).
- Kerr, R. *et al.* Optical imaging of calcium transients in neurons and pharyngeal muscle of *C. elegans*. *Neuron* **26**, 583–594 (2000).
- Hilliard, M.A. *et al.* *In vivo* imaging of *C. elegans* ASH neurons: cellular response and adaptation to chemical repellents. *EMBO J.* **24**, 63–72 (2005).
- Feng, Z., Cronin, C.J., Wittig, J.H., Jr., Sternberg, P.W. & Schafer, W.R. An imaging system for standardized quantitative analysis of *C. elegans* behavior. *BMC Bioinformatics [online]* **5**, 115 (2004) (doi:10.1186/1471-2105-5-115).
- Chung, S.H., Clark, D.A., Gabel, C.V., Mazur, E. & Samuel, A.D. The role of the AFD neuron in *C. elegans* thermotaxis analyzed using femtosecond laser ablation. *BMC Neurosci. [online]* **7**, 30 (2006) (doi:10.1186/1471-2202-7-30).
- Faumont, S. & Lockery, S.R. The awake behaving worm: simultaneous imaging of neuronal activity and behavior in intact animals at millimeter scale. *J. Neurophysiol.* **95**, 1976–1981 (2006).
- Hedgecock, E.M. & Russell, R.L. Normal and mutant thermotaxis in the nematode *Caenorhabditis elegans*. *Proc. Natl. Acad. Sci. USA* **72**, 4061–4065 (1975).
- Hutchison, V.H. & Maness, J.D. The role of behavior in temperature acclimation and tolerance in ectotherms. *Integ. Compar. Biol.* **19**, 367–384 (1979).
- Satterlee, J.S. *et al.* Specification of thermosensory neuron fate in *C. elegans* requires *txx-1*, a homolog of *otd/Otx*. *Neuron* **31**, 943–956 (2001).
- Mori, I. & Ohshima, Y. Neural regulation of thermotaxis in *Caenorhabditis elegans*. *Nature* **376**, 344–348 (1995).
- Kimura, K.D., Miyawaki, A., Matsumoto, K. & Mori, I. The *C. elegans* thermosensory neuron AFD responds to warming. *Curr. Biol.* **14**, 1291–1295 (2004).
- Clark, D.A., Biron, D., Sengupta, P. & Samuel, A.D.T. The AFD sensory neurons encode multiple functions underlying thermotactic behavior in *C. elegans*. *J. Neurosci.* **26**, 7444–7451 (2006).
- Samuel, A.D., Silva, R.A. & Murthy, V.N. Synaptic activity of the AFD neuron in *Caenorhabditis elegans* correlates with thermotactic memory. *J. Neurosci.* **23**, 373–376 (2003).
- Ryu, W.S. & Samuel, A.D. Thermotaxis in *Caenorhabditis elegans* analyzed by measuring responses to defined thermal stimuli. *J. Neurosci.* **22**, 5727–5733 (2002).
- Murakami, H., Bessinger, K., Hellmann, J. & Murakami, S. Aging-dependent and -independent modulation of associative learning behavior by insulin/insulin-like growth factor-1 signal in *Caenorhabditis elegans*. *J. Neurosci.* **25**, 10894–10904 (2005).
- Mohri, A. *et al.* Genetic control of temperature preference in the nematode *Caenorhabditis elegans*. *Genetics* **169**, 1437–1450 (2005).
- Colosimo, M.E. *et al.* Identification of thermosensory and olfactory neuron-specific genes via expression profiling of single neuron types. *Curr. Biol.* **14**, 2245–2251 (2004).
- Matsuki, M., Kunitomo, H. & Iino, Y. $G_{\alpha q}$ regulates olfactory adaptation by antagonizing $G_{\alpha q}$ -DAG signaling in *Caenorhabditis elegans*. *Proc. Natl. Acad. Sci. USA* **103**, 1112–1117 (2006).
- Sakane, F., Imai, S., Yamada, K. & Kanoh, H. The regulatory role of EF-hand motifs of pig 80K diacylglycerol kinase as assessed using truncation and deletion mutants. *Biochem. Biophys. Res. Commun.* **181**, 1015–1021 (1991).
- Yamada, K., Sakane, F., Matsushima, N. & Kanoh, H. EF-hand motifs of α , β and γ isoforms of diacylglycerol kinase bind calcium with different affinities and conformational changes. *Biochem. J.* **321**, 59–64 (1997).
- Sakane, F., Yamada, K., Imai, S. & Kanoh, H. Porcine 80-kDa diacylglycerol kinase is a calcium-binding and calcium/phospholipid-dependent enzyme and undergoes calcium-dependent translocation. *J. Biol. Chem.* **266**, 7096–7100 (1991).
- Sanjuan, M.A., Jones, D.R., Izquierdo, M. & Merida, I. Role of diacylglycerol kinase α in the attenuation of receptor signaling. *J. Cell Biol.* **153**, 207–220 (2001).
- Sakane, F., Kai, M., Wada, I., Imai, S. & Kanoh, H. The C-terminal part of diacylglycerol kinase α lacking zinc fingers serves as a catalytic domain. *Biochem. J.* **318**, 583–590 (1996).
- van Blitterswijk, W.J. & Houssa, B. Properties and functions of diacylglycerol kinases. *Cell. Signal.* **12**, 595–605 (2000).
- Miyawaki, A. *et al.* Fluorescent indicators for Ca^{2+} based on green fluorescent proteins and calmodulin. *Nature* **388**, 882–887 (1997).
- Coburn, C. & Bargmann, C.I. A putative cyclic nucleotide-gated channel is required for sensory development and function in *C. elegans*. *Neuron* **17**, 695–706 (1996).
- Komatsu, H., Mori, I. & Ohshima, Y. Mutations in a cyclic nucleotide-gated channel lead to abnormal thermosensation and chemosensation in *C. elegans*. *Neuron* **17**, 707–718 (1996).
- Hofmann, T. *et al.* Direct activation of human TRPC6 and TRPC3 channels by diacylglycerol. *Nature* **397**, 259–263 (1999).

39. Nishizuka, Y. Intracellular signaling by hydrolysis of phospholipids and activation of protein C. *Science* **258**, 607–614 (1992).
40. Estacion, M., Sinkins, W.G. & Schilling, W.P. Regulation of *Drosophila* transient receptor potential-like (TrpL) channels by phospholipase C-dependent mechanisms. *J. Physiol. (Lond.)* **530**, 1–19 (2001).
41. Maruyama, H., Rakow, T.L. & Maruyama, I.N. Synaptic exocytosis and nervous system development impaired in *Caenorhabditis elegans unc-13* mutants. *Neuroscience* **104**, 287–297 (2001).
42. Richmond, J.E., Davis, W.S. & Jorgensen, E.M. UNC-13 is required for synaptic vesicle fusion in *C. elegans*. *Nat. Neurosci.* **2**, 959–964 (1999).
43. Raghuram, P. *et al.* Constitutive activity of the light-sensitive channels TRP and TRPL in the *Drosophila* diacylglycerol kinase mutant, *rdgA*. *Neuron* **26**, 169–179 (2000).
44. Hazel, J.R. & Williams, E.E. The role of alterations in membrane lipid composition in enabling physiological adaptation of organisms to their physical environment. *Prog. Lipid Res.* **29**, 167–227 (1990).
45. Cossins, A.R. Homeoviscous adaptation of biological membranes and its functional significance. In *Temperature Adaptation of Biological Membranes* (ed. Cossins, A.R.) 63–76 (Portland, London, 1994).
46. Okochi, Y., Kimura, K.D., Ohta, A. & Mori, I. Diverse regulation of sensory signaling by *C. elegans* nPKC-epsilon/eta TTX-4. *EMBO J.* **24**, 2127–2137 (2005).
47. Nurrish, S., Segalat, L. & Kaplan, J.M. Serotonin inhibition of synaptic transmission: $G\alpha_0$ decreases the abundance of UNC-13 at release sites. *Neuron* **24**, 231–242 (1999).
48. Inada, H. *et al.* Identification of guanylyl cyclases that function in thermosensory neurons of *Caenorhabditis elegans*. *Genetics* **172**, 2239–2252 (2006).
49. Kuhara, A., Inada, H., Katsura, I. & Mori, I. Negative regulation and gain control of sensory neurons by the *C. elegans* calcineurin TAX-6. *Neuron* **33**, 751–763 (2002).
50. Gomez, M. *et al.* Ca^{2+} signaling via the neuronal calcium sensor-1 regulates associative learning and memory in *C. elegans*. *Neuron* **30**, 241–248 (2001).